Time variations of descent in the Antarctic vortex during the early winter of 1997

AUTHOR(S):

Kawamoto, Nozomi; Kanzawa, Hiroshi; Shiotani, Masato

CITATION:

Kawamoto, Nozomi ...[et al]. Time variations of descent in the Antarctic vortex during the early winter of 1997. Journal of Geophysical Research: Atmospheres 2004, 109(D18): D18309.

ISSUE DATE:

2004-09

URL:

http://hdl.handle.net/2433/217796

JOURNAL OF GEOPHYSICAL RESEARCH, VOL. 109, D18309, doi:10.1029/2004JD004650, 2004

Time variations of descent in the Antarctic vortex during the early winter of 1997

Nozomi Kawamoto
Earth Observation Research and Application Center, Japan Aerospace Exploration Agency, Tokyo, Japan

Hiroshi Kanzawa[1]
National Institute for Environmental Studies, Ibaraki, Japan

Masato Shiotani
Research Institute for Sustainable Humanosphere, Kyoto University, Kyoto, Japan

Received 16 February 2004; revised 3 June 2004; accepted 25 June 2004; published 23 September 2004.

[1] We analyzed long-lived chemical constituents observed by the Improved Limb Atmospheric Spectrometer (ILAS) on board the Advanced Earth Observing Satellite (ADEOS) to study the stratospheric descent in the Southern Hemisphere polar vortex. The ILAS N_2O distribution inside the polar vortex exhibited clear downward motion in February to June 1997. Average descent for the 5 months is estimated to be ~2.1–1.7 km month^{-1} in the middle stratosphere. In late April to June when planetary waves are relatively active, the vertical velocity displays time variations with a period of about 10 days. These time variations also synchronize with both time variations of the temperature time change ($\partial\overline{T}/\partial t$) and the Eliassen-Palm flux divergence (D_F) in high latitudes. Moreover, a correlation coefficient map in the latitude-height cross section between the vertical velocity and the temperature time change reveals an interesting four-box pattern, suggesting warming below 10 hPa and cooling above 10 hPa in the polar region (70°–90°S) and an opposite distribution in midlatitudes (40°–70°S), when large descent is observed inside the polar vortex. It is just like the meridional circulation in response to D_F induced by planetary waves, which was first illustrated by Matsuno's stratospheric sudden warming theory. *INDEX TERMS:* 0341 Atmospheric Composition and Structure: Middle atmosphere—constituent transport and chemistry (3334); 3334 Meteorology and Atmospheric Dynamics: Middle atmosphere dynamics (0341, 0342); 3360 Meteorology and Atmospheric Dynamics: Remote sensing; *KEYWORDS:* ILAS, polar vortex, descent rate, transport, trace species, Southern Hemisphere

Citation: Kawamoto, N., H. Kanzawa, and M. Shiotani (2004), Time variations of descent in the Antarctic vortex during the early winter of 1997, *J. Geophys. Res.*, *109*, D18309, doi:10.1029/2004JD004650.

1. Introduction

[2] The Lagrangian circulation plays important roles in the stratospheric polar dynamics and chemistry. The circulation (usually "zonal mean" circulation) has been mainly estimated using net radiative heating based on the transformed Eulerian-Mean (TEM) equations [e.g., *Rosenfield et al.*, 1994]. The Upper Atmosphere Research Satellite (UARS) launched in September 1991 observed global distributions of long-lived atmospheric constituents, providing a powerful way for estimating the Lagrangian circulation directly in terms of tracer transport. In particular, the Halogen Occultation Experiment (HALOE) on board UARS measured long-lived minor gases with a high vertical resolution for over 10 years. This estimation is generally useful in the Southern Hemisphere (SH) polar vortex, because the strong westerly jet isolates the air inside the polar vortex from the outside, that is, the horizontal mixing through the vortex edge is expected to be small. From analyses of the HALOE methane (CH_4), *Russell et al.* [1993] first demonstrated clear descent motion inside the SH polar vortex, and *Schoeberl et al.* [1995] calculated the net winter descent of 1992 in the middle and lower stratosphere (1.8 km month^{-1} at the CH_4 mixing ratio of 0.4–0.8 ppmv). Recently, *Kawamoto and Shiotani* [2000] revealed a large interannual variability of net winter descent (1.2–1.8 km month^{-1}) in 1992–1997 at the CH_4 mixing ratio of 0.6 ppmv, corresponding to the middle stratosphere. Using carbon monoxide (CO) observed by the Improved Stratospheric And Mesospheric Sounder (ISAMS) on board UARS, *Allen et al.* [2000] reported a rapid descent (7.6–10.0 km month^{-1}) in the

[1]Now at Department of Earth and Environmental Sciences, Graduate School of Environmental Studies, Nagoya University, Nagoya, Japan.

0148-0227/04/2004JD004650

upper stratosphere from April to May 1992. *Nedoluha et al.* [2000] also described a descent in the stratosphere from water vapor (H_2O) observed by POAM III. *Abrams et al.* [1996] calculated both a slow descent in the lower stratosphere (0.5–1.5 km month^{-1}) and a rapid descent in the middle and upper stratosphere (2.5–3.5 km month^{-1}) in November 1994 from long-lived tracers observed by the atmospheric trace molecule spectroscopy (ATMOS), the shuttle-borne high-resolution Fourier transform infrared spectroscopy (FTIR) instrument.

[3] The Improved Limb Atmospheric Spectrometer (ILAS) on board the Advanced Earth Observing Satellite (ADEOS) had measured stratospheric minor constituents and aerosols in both polar regions for 8 months (November 1996 to June 1997). Trace gases observed by ILAS have a high vertical resolution (~2 km) and are expected to describe daily variations of vertical motions in high latitudes. The objective of this study is to estimate the descent rate inside the SH polar vortex in the early winter of 1997 using ILAS trace gas data of nitrous oxide (N_2O) and CH_4, and discuss short time variations (a period of ~10 days) seen in the descent rate. Most of the results in this paper are based on N_2O analyses because the data quality of ILAS N_2O is generally better than that of ILAS CH_4 in the winter stratosphere (see section 2).

[4] N_2O is a long-lived tracer in the stratosphere and is treated as an inert and passive tracer for the present purposes. The chemical lifetime of N_2O in high latitudes is sufficiently long at its minimum for the present analysis (i.e., over 10^7 s (~4 months) even at 1000 K (~34 km) in midsummer high latitudes), and is very long at its maximum (i.e., over 10^9 s (~30 years) at 400 K (~12 km) in midwinter high latitudes) [*Solomon et al.*, 1986]. CH_4 is also a long-lived tracer, and its chemical lifetime generally exceeds that of N_2O in the stratosphere. The lifetime in high latitudes is over $10^{7.25}$ s (~7 months) at 1000 K (~34 km) in midsummer [*Solomon et al.*, 1986]. Strong vertical gradients of CH_4, required for estimating vertical velocities precisely, are located higher in altitude than those of N_2O.

[5] A close relationship between the descent rate in the SH polar vortex and the planetary wave activity in winter on a seasonal average basis has been reported by *Kawamoto and Shiotani* [2000], suggesting years with larger (smaller) descent for years with larger (smaller) planetary wave activity. In this study, we will focus on short time variations on the order of days seen in the vertical velocity related to planetary wave events in early winter, which are relatively small events compared with the stratospheric sudden warmings, but have basically the same dynamical mechanism as the sudden warmings in terms of the planetary wave-mean flow interaction.

[6] This paper is organized as follows. Section 2 explains the ILAS and UKMO data we used. Section 3 describes the ILAS N_2O data with the UKMO meteorological fields in the SH for November 1996 to June 1997. Some dynamical events from the ILAS N_2O field over the SH high latitudes can be depicted. Section 4 estimates the polar vortex-averaged descent and discusses short time variations on the order of days, which planetary-scale waves have, in the vertical velocity. Section 5 presents the summary and discussion.

2. Data and Analyses

2.1. ILAS

[7] In this study, we analyze ILAS data processed with the version 6.00 algorithm in early SH winter of 1997 (February to June). The ILAS instrument is described briefly by *Sasano et al.* [1999] and intensively by *Nakajima et al.* [2002a]. The ILAS version 5.20 algorithm is detailed by *Yokota et al.* [2002] and *Nakajima et al.* [2002b]. ILAS obtained about 14 solar occultation measurements per day during sunrise for the Northern Hemisphere (NH) and another about 14 measurements during sunset for the SH. The measurements were made approximately along a latitude circle for both events. The sunset measurements occurred in the latitude range of 88°–65°S for the period we analyzed (Figure 1a). The data are available at altitude levels for the range of ~10–50 km with a vertical spacing of 1 km. The data quality of ILAS version 5.20 N_2O for the altitude range concerned in this study, i.e., 400–1000 K potential temperature levels (corresponding altitudes of ~12–34 km), is sufficient for the present purposes [*Kanzawa et al.*, 2003]. The data quality of ILAS version 5.20 CH_4 for the altitude range concerned, i.e., 30–50 km, is sufficient in the winter upper stratosphere [*Kanzawa et al.*, 2003]. The data quality of the ILAS version 6.00 N_2O and CH_4 used in the present study is slightly better than that of version 5.20.

2.2. UKMO

[8] We analyzed the UKMO assimilation data to investigate dynamical fields [*Swinbank and O'Neill*, 1994]. The globally analyzed fields are mapped on a 2.5° × 3.75° latitude-longitude grid at 22 pressure levels (1000–0.3 hPa), with a vertical spacing of about 2.7 km. Ertel's potential vorticity (PV) on isentropic surfaces is calculated using the UKMO data. Moreover, the ILAS trace gas data and the UKMO horizontal wind are rearranged in the PV-based equivalent latitude (EL) coordinates [*Butchart and Remsberg*, 1986] to distinguish ILAS gas profiles inside the polar vortex from those outside. The EL coordinate is thus useful for understanding the tracer distribution when the polar vortex is observed in a winter hemisphere.

2.3. Transformed-Eulerian Mean Framework

[9] The set of quasi-geostrophic TEM equations on a sphere is helpful for understanding the relationship between vertical flows and meteorological fields. The zonal mean momentum equation, thermodynamic equation, and continuity equation of the quasi-geostrophic TEM set are as follows [*Andrews et al.*, 1987]:

$$\partial\overline{u}/\partial t - f_0\overline{v^*} - \overline{X} = (\rho_0 a\cos\phi)^{-1}\nabla\cdot\mathbf{F} \equiv D_F, \tag{1}$$

$$\partial\overline{T}/\partial t + N^2 H R^{-1}\overline{w^*} = \overline{J}/c_p, \tag{2}$$

$$(a\cos\phi)^{-1}\partial\left(\overline{v^*}\cos\phi\right)/\partial\phi + \rho_0^{-1}\partial\left(\rho_0\overline{w^*}\right)/\partial z = 0. \tag{3}$$

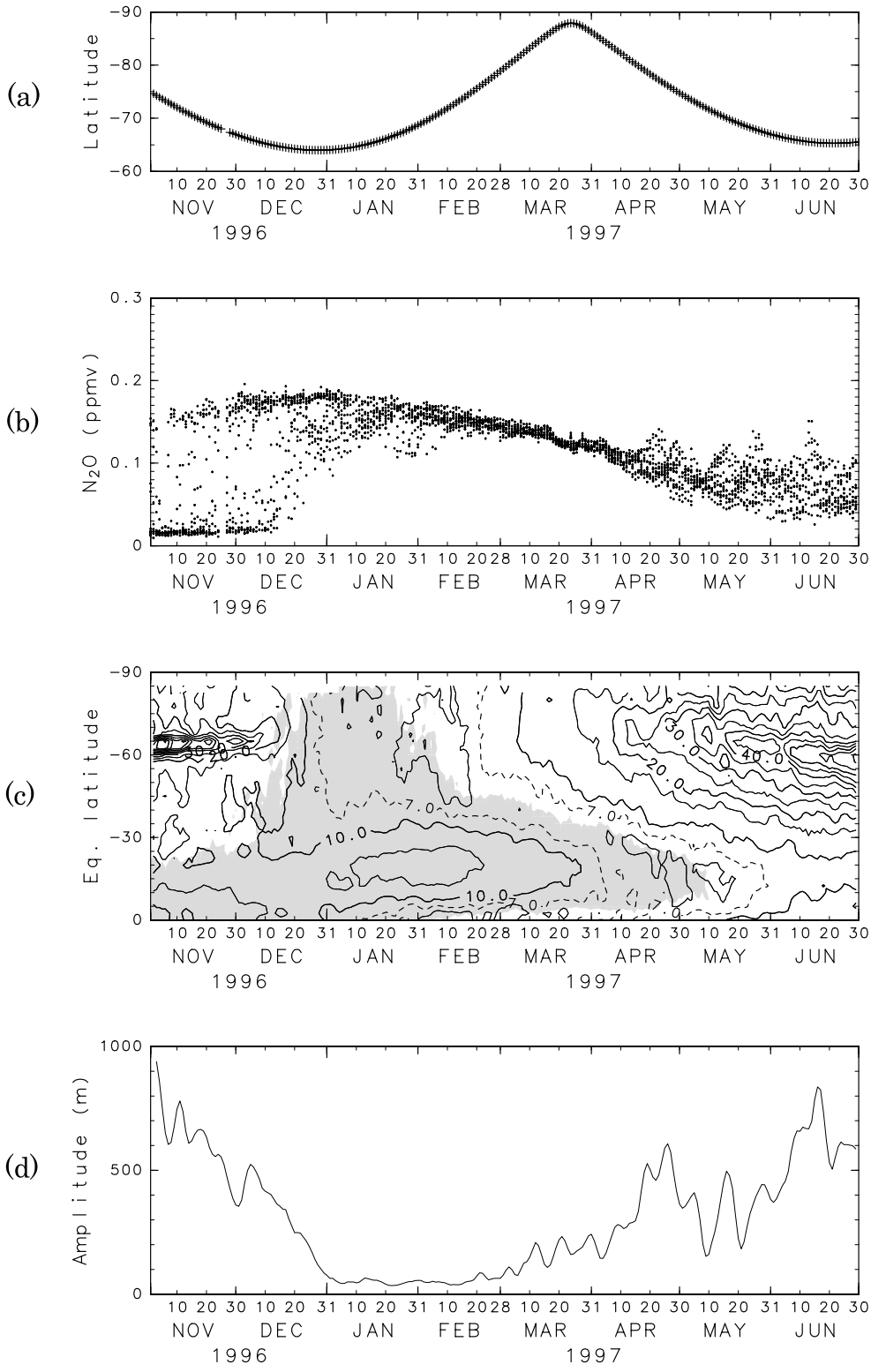

Figure 1. (a) Latitude progression of the ILAS measurement for 8 months. (b) ILAS N_2O distribution on the 600 K (∼23 km) isentropic surface. (c) Time-EL section of horizontal wind defined by $(u^2 + v^2)^{1/2}$ on 600 K (contour interval 5 m s^{-1}; easterly wind areas ($u < 0$) are shaded). (d) Amplitudes of geopotential height (zonal wave number 1–6) at 10 hPa (∼30 km) and 60°S in geographical latitude.

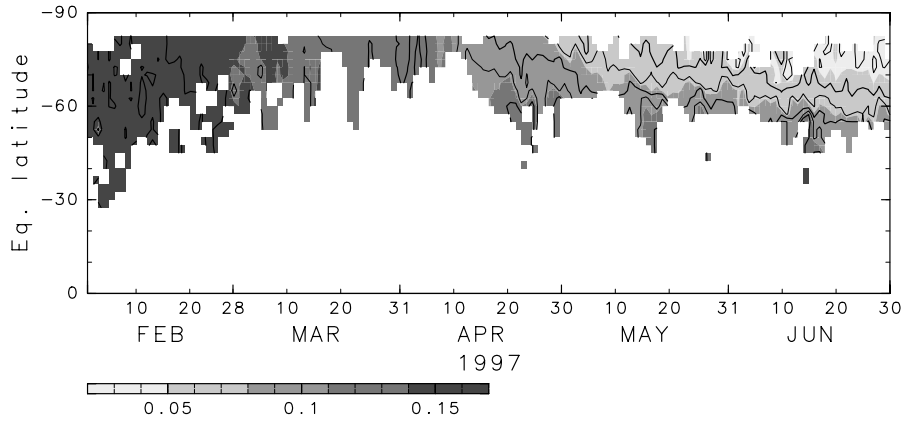

Figure 2. Time-EL section of N_2O on 600 K (contour interval 0.015 ppmv; latitude bin 10°).

We also follow notations as in *Andrews et al.* [1987]. The residual mean meridional circulation ($\overline{v}^*$,$\overline{w}^*$) closely approximates the Lagrangian mean circulation [*Dunkerton*, 1978]. To calculate the Eliassen-Palm flux (**F**; hereafter E-P flux) and its divergence (D_F) as defined in equation (1), we arranged the UKMO data in the form of a zonal mean value and zonal Fourier coefficients (wave number 1–6).

[10] In this study, we will estimate polar vortex-averaged descent and regard the descent as $\overline{w}^*$ in equation (2) when we discuss the relationship between the descent and planetary wave activity represented by the term D_F in equation (1).

3. ILAS N_2O Measurement in the Antarctic

[11] In order to find a suitable period and method for estimating the descent rate in the SH polar vortex, we first discuss dynamical events reflected in the ILAS N_2O field during its 8-month continuous observation. Figure 1 shows the ILAS N_2O observations and UKMO meteorology fields in the SH lower stratosphere. ILAS began operating in November 1996. In November, we can see the strong westerly jet that remained at 600 K (∼23 km) in the EL range of 70°–60°S (Figure 1c). The ILAS N_2O mixing ratio at 600 K (Figure 1b) has two clusters of ∼0.01–0.02 ppmv and ∼0.17–0.19 ppmv. Trace gases have large differences in their mixing ratios between inside and outside the polar vortex because the strong westerly jet prevents the air from mixing through the edge of the polar vortex [e.g., *Schoeberl et al.*, 1992]. The large differences in the N_2O mixing ratios suggest that ILAS observations around a latitude circle caught both air inside (∼0.01–0.02 ppmv) and outside (∼0.17–0.19 ppmv) the polar vortex, which is generally deformed by planetary waves.

[12] In late December 1996, the polar vortex broke up. The westerly jet disappeared suddenly (Figure 1c), and amplitudes of planetary waves decreased as shown in Figure 1d, which illustrates wave amplitudes at 10 hPa (∼30 km) and 60°S in geographic latitude. Simultaneously, the N_2O mixing ratio (Figure 1b) became homogeneous (∼0.15–0.19 ppmv) owing to quasi-horizontal mixing in the Antarctic. After February 1997, the N_2O mixing ratio decreased with time. Because the N_2O mixing ratio becomes smaller with height, the decrease suggests downward motions of the air over the Antarctic. Therefore we can estimate vertical velocities from February to June 1997.

[13] Figure 2 shows the time-EL section at 600 K of the N_2O mixing ratio from February to June. Although the measurements were made approximately along a latitude circle (section 2), ILAS covered wide EL ranges (∼30°) except for late March–early April when the sunset measurement was close to the SH pole (Figure 1a). As also seen in Figure 1b, the mixing ratio decreased with time. It is homogeneous in EL in February–mid-April but decreases toward higher latitudes in late April–June. According to the dynamical fields (Figures 1c and 1d), after mid-April, the westerly jet began to develop and amplitudes of planetary waves increased. As a result, the air inside the strong westerly jet began to be isolated from the outside, while the air in midlatitudes was mixed quasi-horizontally by planetary waves.

[14] To estimate the vertical flow inside the polar vortex, we define the N_2O profiles in the EL range of 90°–70°S as those inside the vortex, because the westerly jet has maxima at ∼70°–60°S EL for late April–June (Figure 1c). Over five N_2O profiles per day represent conditions inside the polar vortex in February–mid-May, except for some days in early February and late March, there were fewer than 5 profiles after late May. The decrease of observation points after late May was caused by an equatorward shift of the ILAS measurement (see Figure 1a). Poor observation numbers in February–mid-April do not affect the estimation of vertical flow because the mixing ratio is homogeneous in EL for this period (Figure 2). However, we need a sufficient number of observation points after mid-April when the mixing ratio has variations in EL (Figure 2). Therefore we checked standard deviations of tracer profiles each day after April to obtain stable values of the mixing ratio averaged in the polar vortex.

[15] Vertical velocities seem to lack uniformity within the polar vortex [*Schoeberl et al.*, 1992; *Rosenfield et al.*, 1994], but there are not enough ILAS measurements to see the horizontal distribution of the descent within the polar vortex for discussing day-to-day variation. Consequently, in the next section, we will discuss the polar vortex-averaged descent flow in February–June, and the relationship between the descent rate and planetary wave activity for late April–June.

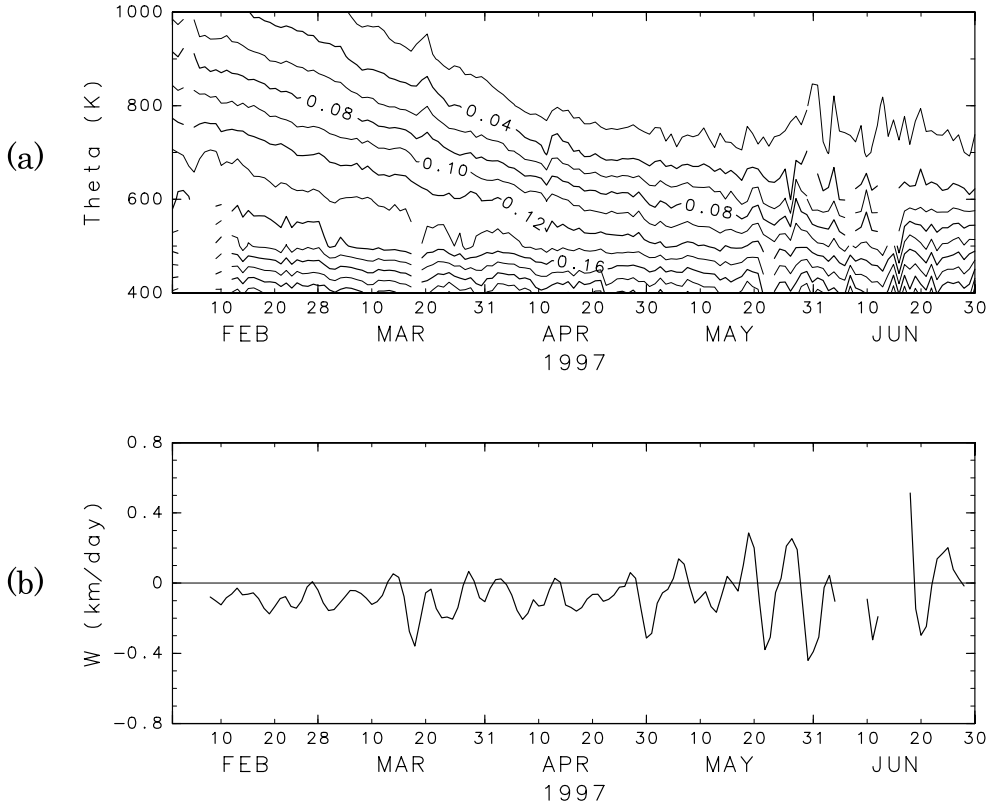

Figure 3. (a) Time-height section of N_2O averaged in EL range of 90°–70°S from 1000 K (∼34 km) to 400 K (∼12 km; contour interval 0.02 ppmv). (b) Vertical velocities estimated from the ILAS N_2O 0.1 ppmv isoline.

[16] In the NH, the planetary wave activity is generally small in early winter. In the SH, however, the amplitudes of planetary waves have two peaks, one in early winter (April–June) and another in late winter (August–October) [*Shiotani et al.*, 1993], and the first peak corresponds to the period we focus on here (late April–June). Fortunately, the peak came earlier in 1997, and planetary waves were rather active compared with other winters of 1992–1996 [see *Kawamoto and Shiotani*, 2000, Figure 8b].

4. Descent in Early Winter of 1997

[17] Figure 3a shows the time-height section of the N_2O mixing ratio inside the polar vortex (averaged over 90°–70°S EL). We can see clear downward motion of isolines from February to June. It is interesting that most isolines began to fall in late summer in the SH (February), as already reported by *Randel et al.* [1998]. Descent rates seem to be rather high in upper levels in February–April. This feature is similar to an estimate based on a radiative transfer model [*Rosenfield et al.*, 1994]. Average descent rates for the 5 months are estimated to be ∼2.1–1.7 km month^{-1} at isolines of 0.04–0.12 ppmv in the middle stratosphere, and they are ∼1.4 km month^{-1} at isolines of 0.14–0.16 ppmv in the lower stratosphere. These rates are somewhat higher than 1.4 (∼35 km) to 1.1 km month^{-1} (∼25 km) averaged for February–October 1997 as estimated by the HALOE CH_4 analysis [*Kawamoto and Shiotani*, 2000] because estimation in this paper focuses on early winter when isolines fall rapidly.

[18] Figure 3b shows vertical velocities estimated by the isoline of 0.1 ppmv, which moves from ∼850 K (∼30 km) to ∼500 K (∼20 km) for 5 months. The averaged descent rate over the 5 months is estimated to be ∼2.1 km month^{-1}. We also found that the vertical velocities exhibit large time variations. The variations are rather small in February–mid-April, except for late March, and become large after late April. The large variation seen in 18–22 March is also found in Figure 1b. During this period, the ILAS measurement is close to the SH pole (Figure 1a), and the ILAS N_2O mixing ratio seems to be unstable for unknown reasons. After late April, however, the variations seem to indicate some robust signals of interest. The variations are observed in wide ELs (Figure 2), and the planetary waves became highly active in this period (Figure 1d). In addition, E-P flux and its divergence reflect relatively active wave events in late April–June as shown in Figure 4. After late April, they have variations with a period of about 10 days, propagating to the equatorial region. This suggests a close relationship between the variations of the vertical velocities and dynamical circulations.

[19] Figure 5 shows the vertical velocity averaged in the polar vortex (the same as in Figure 3b but in units of K d^{-1}), the temperature time change ($\partial\overline{T}/\partial t$; the axis is reversed) in the lower stratospheric polar region (see Figure 5 caption for the detailed location), and the divergence of E-P flux at 10 hPa and 70°S in geographical latitude (the reason for

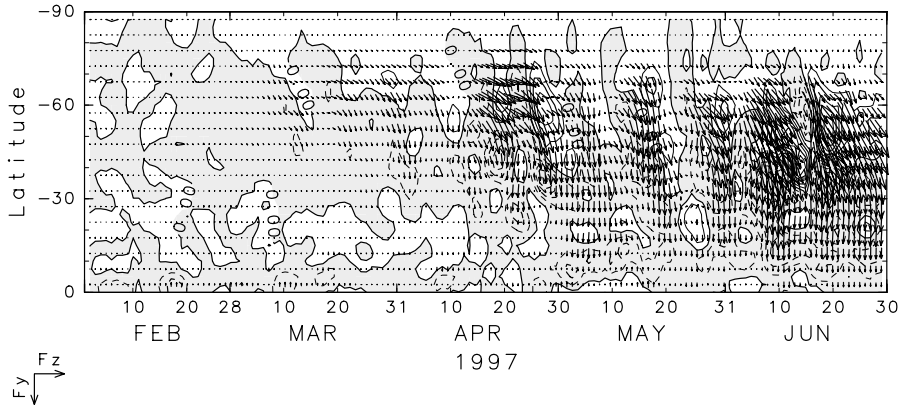

Figure 4. Time-latitude section of the E-P flux vector and its divergence at 10 hPa (contour interval 0.5 m s^{-2}; negative values are shaded). The length of the unit vectors corresponds to 3.0×10^6 kg s^{-2} for the horizontal component (Fy) and $c \times 3.0 \times 10^6$ kg s^{-2} for the vertical component (Fz: the arbitrary factor, c, is set to 125 for drawing the arrows).

choosing this location will be explained in Figure 7) in late April–June. We found that the vertical velocity has large time variations with a period of ~10 days, and synchronizes with variations of the temperature time change and the E-P flux divergence. Such a clear relationship is not seen in February to mid-April (not shown). Figure 5 means that when the descent motion is dominant inside the polar vortex, large negative D_F and positive $\partial\overline{T}/\partial t$ are seen. It conforms exactly to the idea of an atmospheric response to D_F (see equations (1)–(3)). However, amplitudes of the velocity multiplied by a factor of N^2HR^{-1} for comparison with $\partial\overline{T}/\partial t$ (see equation (2)) are rather larger than $\partial\overline{T}/\partial t$ (~6 times). The following are possible explanations of this disagreement on amplitudes. (1) While the ILAS N_2O observation adequately retrieves the phase of the time variations discussed in this paper, it may not precisely retrieve the amplitude of the variations. (2) The thermodynamic equation (equation (2)) has a diabatic heating term ($\overline{J}/c_p$). Figure 3a, where the vertical axis is in theta coordinates, shows vertical variations in the N_2O isolines. This indicates that the diabatic heating, that is, the term $\overline{J}/c_p$ is not zero. It may be negative on average (this problem will be discussed further in the next section). The above conditions also suggest that the correlation coefficient between velocities based on the ILAS N_2O and dynamical fields ($\partial\overline{T}/\partial t$ and D_F) is not so high. This problem with the correlation coefficient seems to appear in the last analysis (Figure 7a).

[20] ILAS also measured the stratospheric CH_4. The ILAS CH_4 is available for 600–1100 K (~23–38 km), and the data quality of ILAS CH_4 above 30 km is sufficient for this study. Figure 6 shows velocities calculated by ILAS CH_4 0.5 ppmv (~29 km; below the 10 hPa level) and 0.2 ppmv (~38 km; above the 10 hPa level). Velocities from CH_4 0.2 ppmv have variations opposite those from CH_4 0.5 ppmv and N_2O 0.1 ppmv isolines. This result is consistent with the picture of a pair of the Lagrangian mean circulation in Matsuno's illustration [*Matsuno*, 1971]; upward and downward motion of the polar air above and below a threshold vertical level related to planetary wave events.

[21] The above results demonstrate the relationships among vertical velocities, the temperature change, and D_F in the polar region. Moreover, a spatial pattern of the

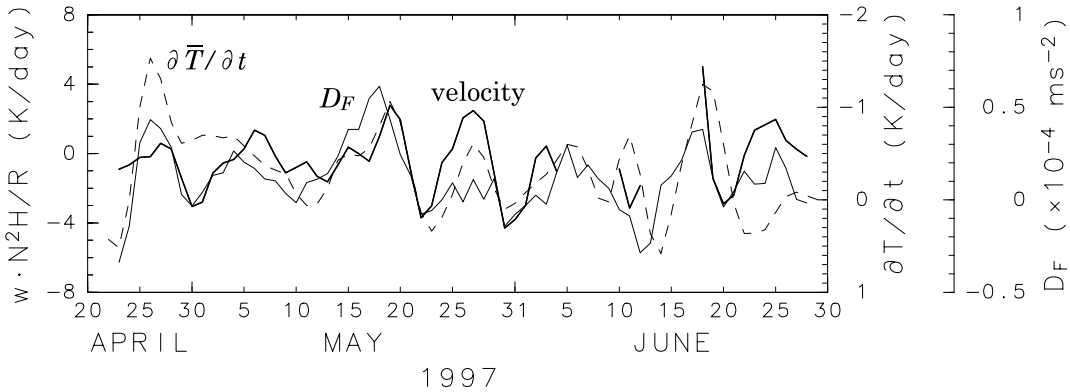

Figure 5. Vertical velocity estimated by the N_2O 0.1 ppmv isoline at ~600–500 K (~23–20 km; thick line). D_F at 10 hPa (~30 km) and 70°S in geographical latitude (thin line). $\partial\overline{T}/\partial t$ at 46.4 hPa (~20 km) from UKMO temperature averaged in 90°–70°S in geographical latitude (dashed thin line: the axis is reversed). A 3-day running mean is applied to the vertical velocity and $\partial\overline{T}/\partial t$, and a 5-day running mean is applied to D_F.

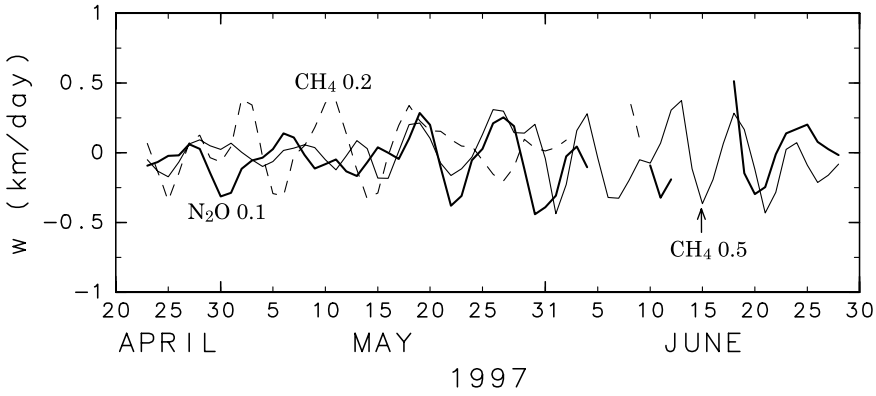

Figure 6. Vertical velocity from the N_2O 0.1 ppmv isoline (∼600–500 K; 23–20 km; thick line), and the ILAS CH_4 0.5 ppmv isoline (∼800 K; 29 km; thin line), and 0.2 ppmv isoline (∼1100 K; 38 km; dashed line). A 3-day running mean is applied to the vertical velocities.

correlation coefficient in the latitude-height section between the vertical velocity and $\partial\overline{T}/\partial t$ also has an interesting feature (Figure 7a). We can see a four-box pattern having negative correlation coefficients below 10 hPa in the polar region (90°–70°S) and above 10 hPa in midlatitudes (70°–40°S), while positive correlation coefficients above 10 hPa in the polar region and below 10 hPa in the midlatitudes. This pattern describes (relative) warmings below 10 hPa and (relative) coolings above 10 hPa in the polar region, and the opposite pattern in the midlatitudes, when the downward motion is relatively large in the lower stratospheric polar vortex. Warming (cooling) suggests downward (upward) motion of the air through adiabatic heating (cooling) in a relative sense. Note that the average vertical velocity is negative (downward) and that the average $\partial\overline{T}/\partial t$ is positive in the region as shown in Figure 5. Therefore the pattern also describes a spatial distribution of (relative) downwelling and (relative) upwelling motions of the air in the domain, which occurred simultaneously with large downward motion inside the polar vortex in the lower stratosphere. It is just like the meridional circulation in response to D_F induced by planetary waves, which was first illustrated by Matsuno's stratospheric sudden warming theory. We also confirmed that amplitudes of D_F having a period of ∼10 days peaked at 10 hPa and 70°–60°S, that is, the center of the four-box pattern (Figure 7b).

[22] Patterns similar to those in Figure 7a were reported by *Randel* [1993], who studied global variations of zonal mean ozone measured by the Solar Backscatter Ultraviolet (SBUV) instrument. During warming events in the NH, the ozone responds dynamically in the lower stratosphere to transport, and photochemically in the upper stratosphere to the circulation-induced temperature changes. *Garcia* [1987] reported temperature and $\overline{w}^*$ changes during stratospheric sudden warmings based on a zonally averaged, quasi-geostrophic TEM model. The circulation in those two

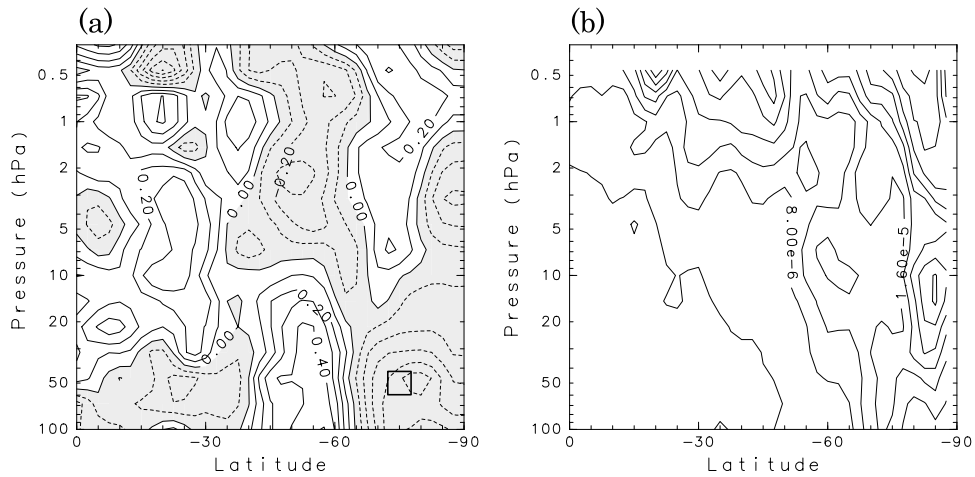

Figure 7. (a) Correlation coefficient between the vertical velocity (N_2O 0.1 ppmv isoline; ∼600–500 K; 23–20 km; reference time series) and $\partial\overline{T}/\partial t$ on each geographical latitude-pressure grid for 20 April to 5 June 1997 (contour interval 0.1; negative values are shaded). The position of the box indicates the approximate region of ILAS measurements used to derive the vertical velocity. (b) Amplitudes of D_F having a period of ∼10 days for 20 April to 5 June 1997 (contour interval 4×10^{-6} m s^{-2}). The amplitudes are calculated using 5-day and 15-day running means; that is, they are derived from components being longer than 5 days and shorter than 15 days.

papers has wider latitude structure than our result (the center of the four-box pattern is ~30° in their papers). This is because they focused on the period when planetary waves are very active (during stratospheric sudden warming events). In fact, using UKMO data, we confirmed that similar patterns seen in temperature fields have wide latitude extent when planetary waves are active in middle to late winter.

5. Summary and Discussion

[23] ILAS on board ADEOS measured atmospheric minor gases in both polar regions from November 1996 to June 1997. Using long-lived tracers (N_2O and CH_4) observed by ILAS, we calculated the Lagrangian vertical velocity inside the SH polar vortex. The ILAS N_2O exhibited some interesting features due to dynamical control in SH winter. The N_2O mixing ratio decreased with time on isentropic surfaces in the lower stratosphere, suggesting the downward diabatic motion of the air inside the polar vortex. We rearranged the ILAS N_2O data based on the EL coordinates, and confirmed that the N_2O distribution inside the polar vortex had clear downward motion in February–June 1997. N_2O isolines fall rapidly in upper levels in February–April. This result is similar to the previous model study. The average descent rate is estimated to be ~2.1–1.4 km month^{-1} at isolines of 0.04–0.16 ppmv during the 5 months of February–June 1997.

[24] Short time variations of vertical velocity from N_2O synchronized with dynamical fields are also found in late April–June. The variations with a period of ~10 days have a consistent relationship with the temperature time change ($\partial\overline{T}/\partial t$) and the divergence of E-P flux (D_F) in view of planetary wave-mean flow interaction. In addition, vertical velocities estimated by ILAS CH_4 also provided evidence of the reliability of the ILAS N_2O variations. It demonstrates that variations of velocities above 10 hPa, around the threshold vertical level of D_F maximum, from ILAS CH_4 are opposite to those below the 10 hPa level from ILAS N_2O.

[25] The relationship in Figure 5 agrees with the picture based on the framework of the TEM equations, but amplitudes of the velocity field are rather large compared with those of $\partial\overline{T}/\partial t$ (~6 times). We discussed some possible reasons in section 4. As one of the reasons, we mentioned the existence of the diabatic heating term $\overline{J}/c_p$ of the thermodynamic equation. According to Figure 3a, N_2O isolines fall across the constant theta lines for February–June, that is, the average diabatic heating term is negative during the 5 months. We also found that N_2O isolines in late April–June varied with the period of ~10 days in the theta coordinate. We calculated diabatic heating using the theta time change ($D\theta/Dt$) along the N_2O isoline of 0.1 ppmv based on the equation $D\theta/Dt = \overline{J}/c_p \exp(\kappa z/H)$ [*Andrews et al.*, 1987], and confirmed that amplitudes of $N^2HR^{-1}\overline{w^*}$ in Figure 5 balanced with those of the diabatic heating instead of small amplitudes of $\partial\overline{T}/\partial t$. This result seems to satisfy the thermodynamic equation (equation (2)), but it is difficult to accept this result as the cause of the disagreement of amplitudes with respect to the period of ~10 days in Figure 5 for the following two reasons. First, the radiative relaxation time (τ) is generally ~30 days in the lower stratosphere. Therefore the period of ~10 days seen in the calculated $\overline{J}/c_p$ is quite short. Second, in late April–June, we found that a four-box pattern may be induced by downward (upward) motion of the air through adiabatic heating (cooling). This means that time variations of ~10 days in N_2O isolines are rather related to the adiabatic heating. It seems reasonable to conclude that amplitudes of $\overline{w^*}$ estimated from ILAS N_2O isolines in late April–June are larger than those of the real atmosphere.

[26] We also analyzed the spatial pattern of the correlation coefficients between the vertical velocity (N_2O 0.1 ppmv isoline; reference time series) and $\partial\overline{T}/\partial t$ of each geographical latitude-pressure grid, both having time variations with a period of ~10 days. The correlation exhibits a four-box pattern of the meridional circulation described by the planetary wave-zonal flow interaction theory. Specifically, when descent is large in the polar vortex, we can see warming below the 10 hPa level and (relative) coolings above the 10 hPa level in the polar region (90°–70°S), and the opposite pattern in the midlatitudes (70°–40°S). The amplitudes of D_F with a period of ~10 days also have a maximum at 10 hPa and 70°–60°S, the center of the four-box pattern in the correlation coefficient field between the vertical velocity and $\partial\overline{T}/\partial t$. We therefore conclude that the variations with the period of ~10 days derived from ILAS N_2O and CH_4 are real and reasonable variations, and prove of the mechanism of the wave-mean flow interaction theory [e.g., *Matsuno*, 1971] based on the data from the satellite measurement.

[27] **Acknowledgments.** Special thanks are given to the ILAS project for providing the ILAS data. The authors are also grateful to the U.K. Meteorological Office for providing the meteorological data sets. The GFD-DENNOU Library was used for drawing the figures.

References

Abrams, M. C., et al. (1996), ATMOS/ATLAS 3 observations of long-lived tracers and descent in the Antarctic vortex in November 1994, *Geophys. Res. Lett.*, *23*, 2341–2344.

Allen, D. R., J. L. Stanford, N. Nakamura, M. A. López-Valverde, M. López-Puertas, F. W. Talor, and J. J. Remedios (2000), Antarctic polar descent and planetary wave activity observed in IASMS CO from April to July 1992, *Geophys. Res. Lett.*, *27*, 665–668.

Andrews, D. G., J. R. Holton, and C. B. Leovy (1987), *Middle Atmosphere Dynamics*, 498 pp., Academic, San Diego, Calif.

Butchart, N., and E. E. Remsberg (1986), The area of the stratospheric polar vortex as a diagnostic for tracer transport on an isentropic surface, *J. Atmos. Sci.*, *43*, 1319–1339.

Dunkerton, T. J. (1978), On the mean meridional mass motions of the stratosphere and mesosphere, *J. Atmos. Sci.*, *35*, 2325–2333.

Garcia, R. R. (1987), On the mean meridional circulation of the middle atmosphere, *J. Atmos. Sci.*, *44*, 3599–3609.

Kanzawa, H., et al. (2003), Validation and data characteristics of nitrous oxide and methane profiles observed by the Improved Limb Atmospheric Spectrometer (ILAS) and processed with the version 5.20 algorithm, *J. Geophys. Res.*, *108*(D16), 8003, doi:10.1029/2002JD002458.

Kawamoto, N., and M. Shiotani (2000), Interannual variability of the vertical descent rate in the Antarctic polar vortex, *J. Geophys. Res.*, *105*, 11,935–11,946.

Matsuno, T. (1971), A dynamical model of the stratospheric sudden warming, *J. Atmos. Sci.*, *28*, 1479–1492.

Nakajima, H., et al. (2002a), Characteristics and performance of the Improved Limb Atmospheric Spectrometer (ILAS) in orbit, *J. Geophys. Res.*, *107*(D24), 8213, doi:10.1029/2001JD001439.

Nakajima, H., et al. (2002b), Tangent height registration for the solar occultation satellite sensor ILAS: A new technique for version 5.20 products, *J. Geophys. Res.*, *107*(D24), 8215, doi:10.1029/2001JD000607.

Nedoluha, G. E., R. M. Bevilacqua, K. W. Hoppel, M. Daehler, E. P. Shettle, J. H. Hornstein, M. D. Fromm, J. D. Lumpe, and J. E. Rosenfield (2000), POAM III measurements of dehydration in the Antarctic lower stratosphere, *Geophys. Res. Lett.*, *27*, 1683–1686.

Randel, W. J. (1993), Global variations of zonal mean ozone during stratospheric warming events, *J. Atmos. Sci.*, *50*, 3308–3321.

Randel, W. J., F. Wu, J. M. Russell III, A. Roche, and J. W. Waters (1998), Seasonal cycles and QBO variations in stratospheric CH_4 and H_2O observed in UARS HALOE data, *J. Atmos. Sci.*, *55*, 163–185.

Rosenfield, J. E., P. A. Newman, and M. R. Schoeberl (1994), Computations of diabatic descent in the stratospheric polar vortex, *J. Geophys. Res.*, *99*, 16,677–16,689.

Russell, J. M., III, A. F. Tuck, L. L. Gordley, J. H. Park, S. R. Drayson, J. E. Harries, R. J. Cicerone, and P. J. Crutzen (1993), HALOE Antarctic observations in the spring of 1991, *Geophys. Res. Lett.*, *20*, 719–722.

Sasano, Y., M. Suzuki, T. Yokota, and H. Kanzawa (1999), Improved Limb Atmospheric Spectrometer (ILAS) for stratospheric ozone layer measurements by solar occultation technique, *Geophys. Res. Lett.*, *26*, 197–200.

Schoeberl, M. R., L. R. Lait, P. A. Newman, and J. E. Rosenfield (1992), The structure of the polar vortex, *J. Geophys. Res.*, *97*, 7859–7882.

Schoeberl, M. R., M. Luo, and J. E. Rosenfield (1995), An analysis of the Antarctic Halogen Occultation Experiment trace gas observations, *J. Geophys. Res.*, *100*, 5159–5172.

Shiotani, M., N. Shimoda, and I. Hirota (1993), Interannual variability of the stratospheric circulation in the Southern Hemisphere, *Q. J. R. Meteorol. Soc.*, *119*, 531–546.

Solomon, S., J. T. Kiehl, R. R. Garcia, and W. Grose (1986), Tracer transport by the diabatic circulation deduced from satellite observations, *J. Atmos. Sci.*, *43*, 1603–1617.

Swinbank, R., and A. O'Neill (1994), A stratosphere-troposphere data assimilation system, *Mon. Weather Rev.*, *122*, 686–702.

Yokota, T., H. Nakajima, T. Sugita, H. Tsubaki, Y. Itou, M. Kaji, M. Suzuki, H. Kanzawa, J. H. Park, and Y. Sasano (2002), Improved Limb Atmospheric Spectrometer (ILAS) data retrieval algorithm for version 5.20 gas profile products, *J. Geophys. Res.*, *107*(D24), 8216, doi:10.1029/2001JD000628.

H. Kanzawa, Department of Earth and Environmental Sciences, Graduate School of Environmental Studies, Nagoya University, Nagoya, 464-8601, Japan. (kanzawa@ihas.nagoya-u.ac.jp)

N. Kawamoto, Earth Observation Research and Application Center, Japan Aerospace Exploration Agency, Tokyo, 104-6023, Japan. (nozomi@eorc.jaxa.jp)

M. Shiotani, Research Institute for Sustainable Humanosphere, Kyoto University, Kyoto, 611-0011, Japan. (shiotani@rish.kyoto-u.ac.jp)